

AUTOMATED DETECTION OF LUNG DISEASES (COVID-19) BASED ON X-RAY IMAGES USING A DEEP LEARNING APPROACH

OMAR SEDQI KAREEM^{*,**}, AHMED KHORSHEED AL-SULAIFANIE^{*}

^{*}College of Engineering, University of Duhok, Kurdistan Region-Iraq

^{**}College of Health and Medical Technology-Shekhan, Duhok Polytechnic University, Kurdistan Region-Iraq

(Accepted for Publication: November 27, 2023)

ABSTRACT

COVID-19 pandemic has presented an unprecedented threat to the global public health system. The respiratory tract's epithelial cells which line the airways are the target of the virus's primary attack. Humans are susceptible to respiratory infections caused by it, which can have mild to severe symptoms like coughing, fever, and weakness. However, it has the potential to develop into other lethal diseases and has already been the cause of millions of fatalities. Thus, a precise diagnosis of these disorders is essential in the current healthcare system. Additionally, quicker chain breaks during early identification result in less disease burden on society. Because of a lack of Reverse Transcription Polymerase Chain Reaction (RT-PCR), early illness diagnosis is challenging. Deep learning (DL) models based on radiographic images could be used to tackle COVID-19. The study offers a Convolutional Neural Network (CNN) model built on a Visual Geometry Group (VGG-16) for classifying and identifying individuals with COVID-19 infection in X-ray chest images. The datasets included 7,245 X-ray images and included 2,898 images for the binary classes and 2,898 images for multi-classes for the model's training and testing. In order to maximize the accuracy of classification, the image enhancement approach was used to highlight important information in the image and minimize some secondary information. Gamma Correction, Histogram Equalization (HE), and Contrast Limited Adaptive Histogram Equalization (CLAHE) were used as three filters for the preprocessing approaches. The suggested model performed most accurately in three classes (97.3% with the use of CLAHE) and the binary class (99.7% with Gamma correction). The system's classification accuracy for lung disorders is higher than that of other DL systems.

KEYWORDS: VGG-16; Convolutional Neural Network; Pneumonia; Deep Learning; X-ray images; COVID-19.

1. INTRODUCTION

A group of viruses that have been referred to as coronaviruses could infect both animals and humans and result in disease. Since protein spikes surround them, such viruses have a crown-like appearance. Those viruses are therefore referred to as coronaviruses (Kumar and Thakur, 2021). In contrast to COVID-19, which

is mostly brought on by the new coronavirus, pneumonia is often brought on by bacterial infections or atypical pathogens like mycoplasma and chlamydia. As a result, COVID-19 is more contagious compared to pneumonia and can be passed from one person to another through direct contact, sneezing, coughing, and other respiratory secretions (Sun et al., 2021). The World Health Organization (WHO)-approved technique for

coronavirus testing is RT-PCR. To rule out coronavirus, some people require multiple tests. The WHO advises that negative lab findings do not exclude viral infection. Due to a lack of COVID-19 screening workstations and testing kits, medical staff are overworked. A significant challenge for medical professionals is promptly and effectively identifying COVID-19 potential patients. As the number of examples increases exponentially, multiple testing is required to comprehend the issue and get to appropriate conclusions (Jain et al., 2020). The COVID-19 RT-PCR test is a laborious procedure that takes at least 4-6 hours to complete from the moment the sample is collected. Radiographic imaging-based technologies, like Computed tomography (CT) scans and X-rays, are one of the quickest screening techniques now accessible (Khan et al., 2021). In addition to RT-PCR, X-ray imaging is an inexpensive, low-radiation technique that could be utilized to quickly test COVID-19 in individuals who are displaying symptoms. X-rays are helpful for determining how an infection is spreading within the lungs, creating treatment strategies, caring for patients, and conducting follow-up. Ground-glass opacity, mixed opacity, and consolidation patterns are the radiographic characteristics of COVID-19 infections. Those characteristics are typically bilaterally distributed in the lower lobes of the lungs with a periphery distribution. Patients' conditions have been monitored via X-ray imaging in numerous nations, including China, Spain, and Italy. This is especially true for those in the intensive care unit who might not be stable enough to receive a CT scan (Attar and Rahimzadeh, 2020).

The high rate of disease transmission and severity of COVID-19 cases provide radiologists with considerable challenges. Therefore, developing a useful technique to aid radiologists in identifying fine differences in radiographic patterns for the purpose of COVID-19 identification is imperative (Karthik *et al.*, 2021; Panwar et al., 2020). Artificial Intelligence (AI) is

developing quickly and has already been used in a number of industries, including education, manufacturing, cybersecurity, and logistics. Similar to this, AI is also being used in healthcare, especially through radiological imaging, for detection, diagnosis, and classification of diseases. DL methods are the most widely used method for using AI in the healthcare and medical fields. Radiologists and scientists are investigating DL algorithms for the extraction of imaging features from disease-related CT and X-ray images. By detecting, analyzing, and categorizing patterns in medical image data, DL has significantly enhanced automated disease identification and management (Karar et al., 2020). CNNs are frequently utilized in the DL techniques for the extraction of the features in large quantities. The convolutional method allows the network to process non-linear data. Data is turned into a more abstract and higher-level representation as it moves through each layer. The network gains more knowledge as it develops. Separating information into more layers makes it easier to extract key components and eliminate redundant details. DL often uses larger datasets and deeper, more complicated Neural Networks (NNs) compared to traditional Machine Learning (ML), which is based on smaller datasets (Nigam et al., 2021; Ramachandran and Rangarajan, 2021).

Our suggested model offers the following significant contributions and benefits:

1. to enhance image classification accuracy, reduce distractions, and draw attention to key information. Methods for improving images have included CLAHE, gamma correction, and HE.
2. with the help of VGG-16 architecture, we have created a novel CNN model which could recognize and classify COVID-19 infections in patient X-rays.
3. we were able to reduce the number of the parameters in the VGG-16 model from over 134 million to roughly 25.6 million by lowering the

number of filters in the network's upper levels.

4. The suggested model performs with good accuracy in multiclass (97.3) and binary class (99.77% based on gamma).

The study is set up like follows: section 2 discusses earlier studies on the use of DL for COVID-19 diagnosis. The proposed model architecture and DL techniques utilized to analyze X-ray images of COVID-19 patients are described thoroughly in Part 3. The experimental findings of our system are shown in Section 4 along with a performance comparison to other systems of a similar design, demonstrating the benefits of our approach. Section 5 presents conclusions.

2. RELATED WORKS

Utilizing ML and DL approaches, previous works have effectively created automated diagnostic systems with quick detection times and high performance. Researchers have used CNNs for expediting the analyses and classification of COVID-19 patient images. Current works have used transfer learning (TL) to classify data using cutting-edge CNN models including VGG, ResNet, Xception, DenseNet, MobileNet, and InceptionNet.

According to (J.L. et al., 2022), a computer-aided model using a use of sparse autoencoder and a feed-forward neural network (FFNN) can detect COVID-19 from chest x-ray (CXR) images. With regard to feature extraction, multiple pre-trained networks are combined, outperforming a single CNN. The combination regarding the custom-made Sparse Autoencoder, FFNN, and Xception and InceptionResnetV2 yielded the greatest accuracy of 0.9578 and AUC of 0.9821. A standard segmentation model (ResUNet) enhances model performance in CXR dataset processing step. In the following stage, CNN applies ML for extracting features from the images in the training dataset. The third stage of the process employs ML methods to merge the

retrieved attributes through voting. In this investigation, there were 4310 normal CXR images and 5178 abnormal ones. According to (Seetharaman and Kalaivani, 2022) the suggested model outperforms ML and CNN and achieves accuracy of 99.35%. A hybrid inception model for diagnosing COVID-19 infections has been created by the authors (Perumal et al., 2022) and will help doctors and frontline staff members assess members of the community. The INASNET model, which was enhanced with batch normalization and a dense layer and trained on large datasets, could increase the effectiveness of detection. Model-based CXRs were recommended by (Hasani and Nasiri, 2022), who also used a DenseNet169 DNN for extracting features. The XGBoost technique was then used to classify the retrieved features. According to the experimental findings, the model's accuracy for the 2-class and 3-class classification tasks was 98.23% and 89.70%, respectively. A method for identifying COVID-19, Pneumonia, and Normal that was suggested by the authors of (Sharma et al., 2022) involved using pre-trained MobileNetV-2 and VGG-16 architectures without their fully connected layers (FCLs). The Confidence Fusion approach was utilized to combine such architectures in order to improve classification accuracy on the two accessible data-sets. The overlapping signs and effects on the lungs make a multiclass diagnosis of many pulmonary illnesses possible thanks to this method. The classification accuracy of the proposed approach was 96.48%.

In order to control COVID-19 spread and improve accuracy, (Karnati et al., 2022) offers an end-to-end IoT infrastructure created for remote patient diagnostics throughout a pandemic. The suggested framework consists of 6 steps, the last of which is the creation of a DNN to read X-rays and precisely assess the severity of COVID-19 lung infection. Five databases that are open to the public are used in the study's experiments. The achieved classification accuracy is 96.01%.

CLAHE and the homomorphic transformation filter are used in this work (Shibu George et al., 2023) for extracting characteristics from CXRs for COVID-19 detection. With the use of a deep CNN model inspired by VGG, the processed images are after that divided into three groups (COVID-19, No-Findings, and Pneumonia). The model achieves 98.06% accuracy in the process of the binary classification and 96.56% accuracy in multi-class classification. Through integrating two datasets, each with two classes, the study (Esmi et al., 2023) proposes an approach for multiclass classification of COVID-19, normal, and other pneumonia. For image preprocessing, noisy images are removed using BRISQUE techniques. With the use of fuzzy pooling as opposed to max pooling increases the model's accuracy. To minimize the consequences of data imbalance, weighted multi-class cross-entropy is used, which speeds up learning and reduces overfitting. Experimental results show that the suggested model accuracy is 96.6%. Two simple CNN models are suggested by the authors of (Hussein et al., 2023) for COVID-19 classification from CXR images. In contrast to the other model, which is built for multi-class classification of COVID-19, normal, and pneumonia cases, the first architecture is intended for binary classification of COVID-19 and normal cases. The models' high accuracy rates of 98.55% and 96.83% for binary and three class models, respectively, were reached after they were trained and tested using CXR images. The

model GW-CNNDC presented in this paper (Udayaraju et al., 2023) uses Lung Radiography images to identify COVID-19. An image with a resolution of 255*255 pixels is produced after the images are processed with the use of Enhanced CNN model with RESNET-50 architecture. The COVID-19 impacted areas are after that determined using the Gradient Weighted model. The model has a 97% accuracy rate for binary classification.

3. MATERIAL AND METHODS

3.1 Data-set description

Due to the limited availability of COVID-19 data, we trained our model using a variety of pneumonia, health, and COVID-19 X-ray images from Kaggle. A total of 7245 different X-ray images from Kaggle have been collected from different sources, ranging in size from 240 x 240 to 3480 x 4248. Three CXR images, such as COVID-19, healthy, and pneumonia, were included in Kaggle dataset for multiclass classifications. To expand the number of cases, we combined a dataset (Curated Chest X-Ray Image Data-set for COVID-19 | Kaggle, n.d.; Kaggle.Com, n.d.) containing 576 Covid-19 X-ray images from Kaggle and 1,583 negative images. Images used for training (70% of the data), validating (15%), and testing (15%) were divided up. 4947 training images, 1149 testing images, and 1149 validation images were used to divide the dataset. Tables 1 and 2 display how the data is divided.

Table(1):- Dataset summary for binary classification

| Data-sets | Normal | COVID-19 | Total |
|------------------|---------------|-----------------|--------------|
| Training | 1,108 | 920 | 2,028 |
| Validation | 275 | 200 | 435 |
| Testing | 275 | 200 | 435 |
| Total | 1,578 | 1,320 | 2,898 |

Table(2):- Dataset summary for multi-class classification

| Data-sets | COVID-19 | Normal | Pneumonia | Total |
|------------|----------|--------|-----------|-------|
| Training | 920 | 1,108 | 2,919 | 4,947 |
| Validation | 200 | 275 | 624 | 1,149 |
| Testing | 200 | 275 | 624 | 1,149 |
| Total | 1,320 | 1,578 | 4,167 | 7,245 |

3.2 Data preprocessing

Pre-processing images is mostly used in order to enhance the visual information included in each input image by lowering noise, boosting contrast, removing high or low frequencies, and using other methods. Image enhancement is an essential technique that draws attention to the most important elements of an image while excluding irrelevant ones, thus increasing identification accuracy. The goal is to create objective images that are better suited than the originals for particular uses. Also, one crucial step in data preprocessing is downsizing the X-Ray images. Labels and images in both datasets were scaled to 128x128 dimensions to shorten training time and expenses. Three different

image enhancement approaches were utilized in this investigation; they are briefly covered in the section that follows.

3.2.1 Histogram equalization (HE)

The contrast and color of images are improved by the preprocessing technique known as HE. The range of dark shades is increased and the range of bright tones is decreased with this method, which entails remapping the gray scale of the image depending on its probability distribution. Thus, local features are diminished and image edges and borders are highlighted (Hou et al., 2021; Emmanuel and Revina, 2021). Equations (1) and (2) are used to solve for the cumulative distribution function (cdf) and probability density function (pdf) in this method.

$$pdf / p(A_k) = \frac{n_k}{n}; k = 0, 1, 2, \dots, L-1 \quad (1)$$

$$cdf / p(A_k) = \sum_{j=0}^k p(A_j) = \sum_{j=0}^k \left(\frac{n_j}{n} \right) \quad (2)$$

In which n represent the number of pixels in an image, k represents the grayscale, and n_k represents the number of pixels with gray level of A_k within image A.

3.2.2 Contrast limited adaptive histogram equalization (CLAHE)

HE performs better when used in conjunction with AHE, a technique for image enhancement. AHE produces local contrast and edge enhancement by independently enhancing the contrast of independent patches and regions inside the image. Instead of using global information, this approach can be adjusted to account for local distribution in pixel intensities

(Kuran and Kuran, 2021; Rahman et al., 2020). By employing the same technique as AHE, yet with a threshold value that limits the amount of contrast enhancement inside a selected region, CLAHE generates more realistic-looking images compared to HE. A few areas of X-ray images are saturated by HE, which CLAHE addresses by restricting the contrast enhancement (Manju et al., 2019).

3.2.3 Gamma correction

Gamma correction is a nonlinear approach that alters the saturation of an image by applying to each pixel value. Gamma correction requires nonlinear techniques even though subtraction,

addition, and multiplication are typically done on each pixel. It's important to keep the gamma value (γ) constant because it shouldn't be either too low or too high. Gamma correction might be useful for images that are either too dark or too light. The transformed image appears lighter compared to the original in the case when γ is less than one, and darker than the original when γ is greater than one (Shamila Ebenezer et al., 2022). Equation for gamma correction:

$$g(x) = 255\left(\frac{x}{255}\right)^{\frac{1}{\gamma(x)}} \quad (3)$$

In which x represents the gray scale regarding the original image.

3.3 CNN architecture

CNNs that have been trained for classifying images with the use of convolutional filters. The early layers of CNNs first extract low level features from CXR images, like colors, curves, textures, and edges. The last layer of CNN produces the probability of every one of the classes, and the deeper layers capture high level features (Rasheed et al., 2020). TL is replacing a few layers of a pre-trained network with the use of various dataset in order to adapt it to categorize new classes. TL involves training the remaining layers regarding a network's filters on a new dataset while leaving the initial layers of network's filters unaltered. Due to the small amount of the training data, TL is used in medical imaging. Subsampling, convolution, and FCLs make up a standard CNN architecture (Roy and Chahar, 2022). CNNs employ additional layers like dropout and batching for accelerating training while preventing overfitting. A popular activation function that generates a vector of probability distributions for various classes is called softmax activation. To add nonlinearity to the model, activation functions are utilized (Verma et al., 2021).

3.4 Proposed model

The proposed model for classification and

detection of COVID-19 infection was described in this section. We upgraded the max-pooling, convolutional, and FCLs of the VGG-16 model for feature extraction. For training and testing VGG-16 model, images are scaled down to 128×128 . We changed the number of kernel filters in the first four layers, the number of convolutional layers in each block, reduced from four to two, and added batch normalization and dropout at the block's end. While retaining the same number of blocks in the network, several changes were implemented. In our model, activation and normalization layers, notably the Rectified Linear Unit (ReLU) and a normalization layer, are present in both the FCL and convolutional layer. In order to further improve the performance regarding our model, batch normalization was used to batch-process COVID-19 images in a way that speeds convergence and reduces "gradient explosion." The model is less possibly to have numerical instability and helps in mitigating any problems which might occur from a large gradient throughout training by leveling the input data. The normalization procedure also assures that the model may be generalized to new data and offers more steady updates to its parameters. Those methods enhance our DL model's training stability and accuracy in classifying COVID-19 from medical images. Our suggested model aims to improve the accuracy and speed of training while lowering the model's dependence on initial weights. The output regarding feature extraction layer must be converted to a flattened, 1D layer as the first stage in the classification process. To reduce overfitting, the classification process uses two FCLs with 2048 neurons each and a dropout layer in between. Figure 1 shows how we classify images utilizing a dense layer with two or three neurons (depending on the number of the classes) and the Softmax activation function to determine if a chest condition is normal, pneumonia, or COVID-19.

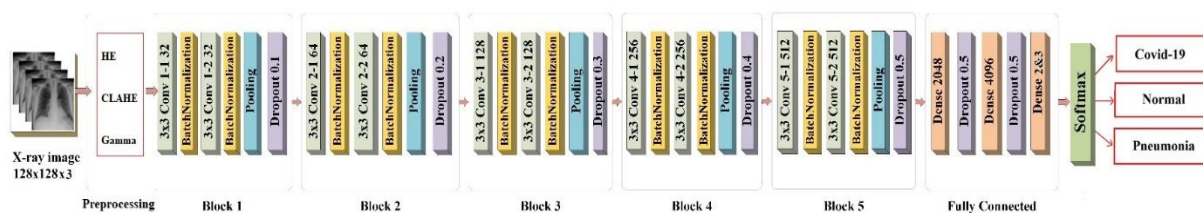


Fig.(1):- The proposed model architecture.

The accuracy of a model throughout training is greatly influenced by hyperparameters. The effectiveness of a model could be impacted by proper hyperparameter value selection. Common hyperparameters in DL models include epoch count, learning rate, the number of dense layers, and batch size. Categorical cross-entropy is typically chosen as the loss function for binary and multi-class classifications. In this method, every one of the classes is given a specific number, and the cross-entropy between actual and predicted label distributions is determined. Due to its computing efficiency, the categorical cross-

entropy loss function is frequently employed in DL for classification tasks. For data belonging to one of the two categories, the cross-entropy function calculates a score which shows average dissimilarity between predicted and real probability distributions, allowing the model to develop the capacity to anticipate outcomes correctly. A key factor in optimizing the training of DL models for classification tasks is the categorical cross-entropy loss function. The computation of average loss is shown in Equation (4). The hyperparameters employed in our model are listed in Table 3.

$$L = -\frac{1}{N} \sum_{i=1}^n (y_i \log(\hat{y}_i) + (1 - y_i) \log(1 - \hat{y}_i)) \quad (4)$$

Table(3):- Hyperparameters of the suggested model

| Hyperparameters | Values |
|---------------------|---------------------------------|
| Learning rate | 0.0010 |
| Optimiser | SGD |
| Epochs | 50 & 100 |
| Batch size | 16 |
| Activation function | Softmax |
| Momentum | 0.95 |
| Loss function | sparse_categorical_crossentropy |

4. RESULTS AND DISCUSSIONS

The model has been trained on a data-set of X-ray images, and performance has been assessed based on multiple measurement criteria parameters to see how well it could identify COVID-19 cases. The tests have been carried out with the use of a laptop with a core i7-5600 U processor running at 2.60 GHz, a NVidia GeForce

840 M 2 GB GPU, and 16 GB of RAM. For classification, a new environment with a number of libraries, like TensorFlow, CV-2, NumPy, Keras, Matplotlib, and Pandas, was built up using anaconda python 3.7 software tool.

4.1 Evaluation and Analysis of Results

Image enhancement is a vital step in image processing process that emphasizes important information in the image while limiting or

removing specific non-essential information to improve the image's ability to be recognized. This is achieved by drawing attention to certain details and changing the images to make them more appropriate for a given application. In our investigation, we used three different techniques for image enhancement. Clip limit and block size are two aspects that should be taken into account while using CLAHE. In both three-class and the binary class classification, we employed a block size of (8x8), a clip limit of 2, and a gamma value of 1.5. We provide the outcomes of the image enhancing approaches for both three-class and binary classifications in the subsection that follows.

4.1.1 Evaluation of binary classification

As filters, three preprocessing methods—gamma correction, CLAHE, and HE—were used. Next, Kaggle datasets with two classes were utilized in order to analyze the suggested model to determine the heterogeneity and robustness of DL models. The suggested end-to-end DL approaches (normal vs. COVID) was used for classifying the CXR images into two classes. The

confusion matrices in Figure 2 indicate the performance regarding the suggested model and the effects of three alternative image enhancing methods. For each of the three strategies, the test dataset included 200 COVID-19 patient images and 235 images of normal patients. The model has been trained for 50 epochs. The outcomes of utilizing HE and CLAHE are depicted in Figures 2(a) and 2(b), respectively, in the confusion matrices. The columns and rows of matrices were filled with the predicted and real instances, accordingly. In both situations, the model correctly classified 199 out of 200 COVID-19 patients and incorrectly classified one as a normal patient. Only one of the 235 normal instances was incorrectly identified in both cases as COVID-19. In the third case, which made use of gamma correction, all 235 normal patients were correctly identified by the model, whereas only one of the 200 COVID-19 patients was misdiagnosed, as seen in Figure 2(c). Table 4 presents the precision, recall, accuracy, and F1-score obtained with the use of image enhancement method.

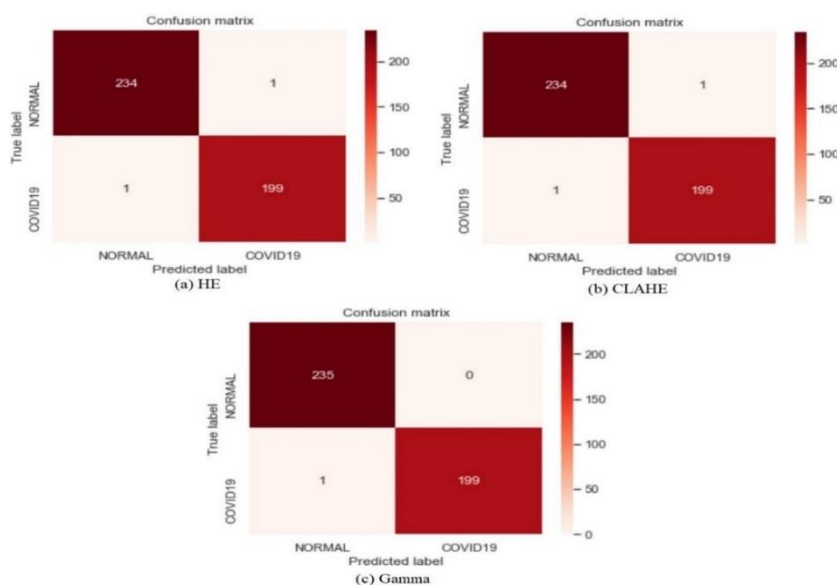


Fig.(2):- Confusion matrix for binary-class using three filter types.

Table(4):- Performance evaluation of the model with the use of image enhancements (binary-class).

| Image enhancements | Case | Evaluation metrics | | | |
|--------------------|----------|--------------------|------------|------|------------|
| | | Recall % | Precision% | F1 % | Accuracy % |
| HE | COVID-19 | 99 | 99 | 99 | 99.54 |
| | Normal | 100 | 100 | 100 | |
| CLAHE | COVID-19 | 99 | 99 | 99 | 99.54 |
| | Normal | 100 | 100 | 100 | |
| Gamma | COVID-19 | 99 | 100 | 100 | 99.77 |
| | Normal | 100 | 100 | 100 | |

4.1.2 Evaluation of three class classification

The three filters stated previously were also used in the research for the three-class classification, and the suggested approach was put to the test for up to 100 epochs. A confusion matrix, which is a matrix that summarizes a classification model's performance, was used to present the results. Figure 3 showed the confusion matrices for each of the three filters that were applied. Out of 275 healthy cases in the first scenario (HE), the multiclass model misclassified eight of them, classifying one as COVID-19 and seven as pneumonia. Additionally, it misclassified two instances of pneumonia and five healthy cases out of 250 COVID-19 cases, failing to distinguish seven of them. 607 images were properly identified as pneumonia by the model, but 17 images were misclassified as normal. Out of 275 normal patients in the second case (CLAHE), the adjusted model

misclassified 19 as pneumonia and none as COVID-19. Furthermore, it misclassified two cases as healthy and three cases as pneumonia out of 250 COVID-19 instances, failing to distinguish five of them. Six of the images have been misclassified as healthy and one as COVID-19, while the model properly identified 617 images as pneumonia. Out of 275 healthy cases in the third case (Gamma), the modified model misclassified 17 of them, classifying 16 of them as pneumonia and one as COVID-19. Additionally, it misclassified three cases as healthy and four cases as pneumonia out of 250 COVID-19 instances, failing to distinguish seven of them. In addition, the model correctly classified 611 images as pneumonia, yet missed 12 healthy images and one COVID-19 image. Table 5 presents the precision, recall accuracy, and F1-score obtained with the use of image enhancement method.

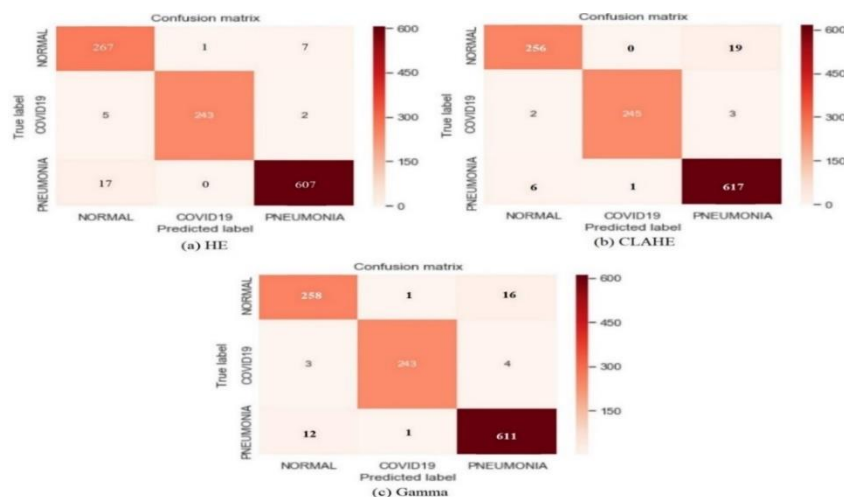


Fig.(3):- fusion matrix for three-class using three filter types.

Table(5):- Performance evaluation of the model with the use of image enhancements (three-class).

| Image enhancements | Case | Evaluation metrics | | | |
|--------------------|-----------|--------------------|------------|-----|-----------|
| | | Recall% | Precision% | F1% | Accuracy% |
| HE | COVID-19 | 97 | 92 | 95 | 97.21 |
| | Normal | 97 | 100 | 98 | |
| | Pneumonia | 97 | 99 | 98 | |
| CLAHE | COVID-19 | 93 | 97 | 95 | 97.3 |
| | Normal | 98 | 100 | 99 | |
| | Pneumonia | 99 | 97 | 98 | |
| Gamma | COVID-19 | 94 | 95 | 94 | 96.77 |
| | Normal | 97 | 99 | 98 | |
| | Pneumonia | 98 | 97 | 97 | |

4.2 DISCUSSION

To prevent and control the spread of COVID-19, rapid quarantine and rapid and early diagnosis are essential. Thus, rapid diagnostic methods are absolutely necessary for pandemic early treatment, detection and isolation. Due to its advantages in speed, accuracy, and ease of use, AI-based models have surpassed conventional techniques in popularity. Compared to CT, using CXR images for COVID-19 and pneumonitis classification has fewer radiation risks, is more accessible, and is more affordable. X-ray images are also cheaper and more widely available than CT scans. DL models might help with early disease detection, and several

works have found that utilizing AI models, COVID-19 pneumonia could be detected with good accuracy. We created a new DL model depending on VGG-16, which has additional feature extraction filters, to classify and detect COVID-19 infections from X-ray images. We also decreased the number of parameters in VGG-16 model from approximately 138 million to 25 million because a CNN model needs a sizable and varied image database to get accurate findings. Our suggested model yields superior outcomes in comparison to earlier investigations. The research on automatic COVID-19 diagnosis from CXR images are summarized in Table 6 along with a comparison to our approach.

Table(6):- Summary of the dataset for multiclass

| Study | Datasets | Architecture | Performance measurement | | | |
|---------------------------------|--|---|-------------------------|---------------|-------------|-------|
| | | | Accuracy % | Sensitivity % | Precision % | F1 % |
| (J.L. et al., 2022) | 504 COVID-19 vs. 542 non-COVID-19 | FFNN | 95.78 | 95.63 | 95.63 | 95.63 |
| (Kalaivani & Seetharaman, 2022) | 5174 COVID-19 vs. 4310 normal | CNN and machine learning for classification | 99.35 | 98.71 | 100 | 99.35 |
| (Perumal et al., 2022) | COVID-19 =183, normal=8066, and pneumonia= 5538. | INASNET | 94.3 | 94 | 94 | 94 |

| | | | | | | |
|-----------------------------|---|---|--|------------------------------|------------------------------|------------------------------|
| (Nasiri & Hasani, 2022) | COVID-19 =125, normal=500, and pneumonia= 500. | DenseNet169 + XGBoost | 89.7 | 95.2 | 92.5 | 91.2 |
| (Sharma et al., 2022) | COVID-19: 1784, Normal: 1755, Pneumonia: 1345 | COVDC-Net | 96.48 | 96.57 | 96.59 | 96.57 |
| (Karnati et al., 2022) | D1 (COVID-19=1625 and non-COVID-19=3783) D2 (COVID-19=1200 and non-COVID-19=134111) D3 (COVID-19=184 and non-COVID-19=3700) D4 (COVID-19=320 and non-COVID-19=445) D5 (COVID-19=125 and non-COVID-19=500) | DNN framework | D1=96.01 D2=96.61 D3= 99.22 D4= 98.83 D5=100 | 96 100 99 99 100 | 96 100 99 98 100 | 96 100 99 99 100 |
| (Shibu George et al., 2023) | COVID-19 =2250 normal=2250, and pneumonia= 2250. | VGG inspired deep CNN | Binary= 98 Multiclass=96.56 | Binary=97 Multiclass=95 | Binary= 97 Multiclass=95 | Binary= 97 Multiclass=95 |
| (Esmi et al., 2023) | COVID-19 = 14270 normal=14208, and pneumonia= 3788 | fuzzy fine-tuned Xception | 96.60 | 94 | 93 | 94 |
| (Hussein et al., 2023) | COVID-19 = 3616 normal=10192, and pneumonia= 1345 | Lightweight CNN Model | 96.83 | - | - | - |
| (Udayaraju et al., 2023) | COVID-19 normal=13808 | GW-CNNDC | 97 | 97.87 | 94 | 90.89 |
| proposed model | X-ray images COVID-19 = 1420, Normal = 1658, Pneumonia = 4167 | Pre-processing (Gamma&CLAHE), Modified VGG-16 | Binary = 99.77 Multi = 97.3 | 99.5 96.7 | 100 98 | 100 97.33 |

5. CONCLUSIONS

Through analyzing CXR images of suspect patients, the research suggests a deep CNN model for COVID-19 classification. The model distinguishes between healthy individuals, those who have the coronavirus, and pneumonia diseases. To improve classification accuracy, an image enhancement method is employed before CNN to draw attention to the image's most important details and to downplay some of the less important ones. For two classes and three classes, three filters—HE, CLAHE, and gamma correction—are used as preprocessing approaches. For two-class and three-class, the model is trained for 50 epochs and 100 epochs, respectively. For the binary test, there were 200 images for COVID-19 patients and 235 for healthy people. The model's accuracy in HE is 99.54%; for CLAHE, it is the same accuracy; however, when gamma was utilized, the accuracy rose to 99.77%. The total number of images used for testing for multiclass was 200 for COVID-19, 275 for normal, and 624 for pneumonia. The model's accuracy in CLAHE it is 97.3%, in the HE is 97.21%, yet when gamma was used the accuracy rose to 96.77%. The recommended CNN approach speeds up treatment and diagnosis while lowering the risk of COVID-19 spread. It also decreases costs and radiation exposure.

Acknowledgments

I want to thank my supervisor, the University of Duhok, and the Duhok Polytechnic University for their assistance in getting the research done. I sincerely appreciate and value the continued guidance and support I have received.

REFERENCES

Chahar, S., & Roy, P. K. (2022). COVID-19: A Comprehensive Review of Learning Models. *Archives of Computational Methods in Engineering: State of the Art Reviews*, 29(3), 1915–1940. [https://doi.org/10.1007/s11831-](https://doi.org/10.1007/s11831-021-09641-3)

021-09641-3

Curated Chest X-Ray Image Dataset for COVID-19 / *Kaggle*. (n.d.). Retrieved August 30, 2021, from

<https://www.kaggle.com/unaisait/curated-chest-xray-image-dataset-for-covid19>

Esmi, N., Golshan, Y., Asadi, S., Shahbahrani, A., & Gaydadjiev, G. (2023). A fuzzy fine-tuned model for COVID-19 diagnosis. *Computers in Biology and Medicine*, 153, 106483. <https://doi.org/https://doi.org/10.1016/j.compbiomed.2022.106483>

Hou, Y., Li, Q., Zhang, C., Lu, G., Ye, Z., Chen, Y., Wang, L., & Cao, D. (2021). The State-of-the-Art Review on Applications of Intrusive Sensing, Image Processing Techniques, and Machine Learning Methods in Pavement Monitoring and Analysis. *Engineering*, 7(6), 845–856.

<https://doi.org/https://doi.org/10.1016/j.eng.2020.07.030>

Hussein, H. I., Mohammed, A. O., Hassan, M. M., & Mstafa, R. J. (2023). Lightweight deep CNN-based models for early detection of COVID-19 patients from chest X-ray images. *Expert Systems with Applications*, 223, 119900. <https://doi.org/https://doi.org/10.1016/j.eswa.2023.119900>

J.L., G., Abraham, B., M.S., S., & Nair, M. S. (2022). A computer-aided diagnosis system for the classification of COVID-19 and non-COVID-19 pneumonia on chest X-ray images by integrating CNN with sparse autoencoder and feed forward neural network. *Computers in Biology and Medicine*, 141, 105134. <https://doi.org/https://doi.org/10.1016/j.compbiomed.2021.105134>

Jain, G., Mittal, D., Thakur, D., & Mittal, M. K. (2020). A deep learning approach to detect Covid-19 coronavirus with X-Ray images. *Biocybernetics and Biomedical Engineering*. <https://doi.org/10.1016/j.bbe.2020.08.008>

kaggle.com. (n.d.). *Kaggle.Com*. <https://www.kaggle.com/prashant268/chest->

- xray-covid19-pneumonia
- Kalaivani, S., & Seetharaman, K. (2022). A three-stage ensemble boosted convolutional neural network for classification and analysis of COVID-19 chest x-ray images. *International Journal of Cognitive Computing in Engineering*, 3, 35–45. <https://doi.org/https://doi.org/10.1016/j.ijcce.2022.01.004>
- Karar, M. E., Hemdan, E. E.-D., & Shouman, M. A. (2020). Cascaded deep learning classifiers for computer-aided diagnosis of COVID-19 and pneumonia diseases in X-ray scans. *Complex & Intelligent Systems*. <https://doi.org/10.1007/s40747-020-00199-4>
- Karnati, M., Seal, A., Sahu, G., Yazidi, A., & Krejcar, O. (2022). A novel multi-scale based deep convolutional neural network for detecting COVID-19 from X-rays. *Applied Soft Computing*, 125, 109109. <https://doi.org/https://doi.org/10.1016/j.asoc.2022.109109>
- Karthik, R., Menaka, R., & Hariharan, M. (2021). Learning distinctive filters for COVID-19 detection from chest X-ray using shuffled residual CNN. *Applied Soft Computing*, 99(xxxx). <https://doi.org/10.1016/j.asoc.2020.106744>
- Khan, S. H., Sohail, A., Zafar, M. M., & Khan, A. (2021). Coronavirus disease analysis using chest X-ray images and a novel deep convolutional neural network. *Photodiagnosis and Photodynamic Therapy*, 35, 102473. <https://doi.org/https://doi.org/10.1016/j.pdpdt.2021.102473>
- Kuran, U., & Kuran, E. C. (2021). Parameter selection for CLAHE using multi-objective cuckoo search algorithm for image contrast enhancement. *Intelligent Systems with Applications*, 12, 200051. <https://doi.org/https://doi.org/10.1016/j.iswa.2021.200051>
- Manju, R. A., Koshy, G., & Simon, P. (2019). Improved Method for Enhancing Dark Images based on CLAHE and Morphological Reconstruction. *Procedia Computer Science*, 165, 391–398. <https://doi.org/https://doi.org/10.1016/j.procs.2020.01.033>
- Nasiri, H., & Hasani, S. (2022). Automated detection of COVID-19 cases from chest X-ray images using deep neural network and XGBoost. *Radiography*, 28(3), 732–738. <https://doi.org/https://doi.org/10.1016/j.radi.2022.03.011>
- Nigam, B., Nigam, A., Jain, R., Dodia, S., Arora, N., & Annappa, B. (2021). COVID-19: Automatic detection from X-ray images by utilizing deep learning methods. *Expert Systems with Applications*, 176, 114883. <https://doi.org/https://doi.org/10.1016/j.eswa.2021.114883>
- Panwar, H., Gupta, P. K., Siddiqui, M. K., Morales-Menendez, R., & Singh, V. (2020). Application of deep learning for fast detection of COVID-19 in X-Rays using nCOVnet. *Chaos, Solitons and Fractals*. <https://doi.org/10.1016/j.chaos.2020.109944>
- Perumal, M., Nayak, A., Sree, R. P., & Srinivas, M. (2022). INASNET: Automatic identification of coronavirus disease (COVID-19) based on chest X-ray using deep neural network. *ISA Transactions*, 124, 82–89. <https://doi.org/https://doi.org/10.1016/j.isatra.2022.02.033>
- Rahimzadeh, M., & Attar, A. (2020). A modified deep convolutional neural network for detecting COVID-19 and pneumonia from chest X-ray images based on the concatenation of Xception and ResNet50V2. *Informatics in Medicine Unlocked*, 19. <https://doi.org/10.1016/j.imu.2020.100360>
- Rahman, T., Chowdhury, M. E. H., Khandakar, A., Islam, K. R., Islam, K. F., Mahbub, Z. B., Kadir, M. A., & Kashem, S. (2020). Transfer learning with deep Convolutional Neural Network (CNN) for pneumonia detection using chest X-ray. *Applied Sciences (Switzerland)*. <https://doi.org/10.3390/app10093233>
- Rangarajan, A. K., & Ramachandran, H. K. (2021). A preliminary analysis of AI based smartphone

- application for diagnosis of COVID-19 using chest X-ray images. *Expert Systems with Applications*, 183, 115401. <https://doi.org/https://doi.org/10.1016/j.eswa.2021.115401>
- Rasheed, A., Younis, S., Bilal, M., & Rasheed, M. (2020). *Classification of Chest Diseases using Wavelet Transforms and Transfer Learning*. Springer, Singapore.
- Revina, I. M., & Emmanuel, W. R. S. (2021). A Survey on Human Face Expression Recognition Techniques. *Journal of King Saud University - Computer and Information Sciences*, 33(6), 619–628. <https://doi.org/https://doi.org/10.1016/j.jksuci.2018.09.002>
- Shamila Ebenezer, A., Deepa Kanmani, S., Sivakumar, M., & Jeba Priya, S. (2022). Effect of image transformation on EfficientNet model for COVID-19 CT image classification. *Materials Today: Proceedings*, 51, 2512–2519. <https://doi.org/https://doi.org/10.1016/j.matpr.2021.12.121>
- Sharma, A., Singh, K., & Koundal, D. (2022). A novel fusion based convolutional neural network approach for classification of COVID-19 from chest X-ray images. *Biomedical Signal Processing and Control*, 77, 103778. <https://doi.org/https://doi.org/10.1016/j.bspc.2022.103778>
- Shibu George, G., Raj Mishra, P., Sinha, P., & Ranjan Prusty, M. (2023). COVID-19 detection on chest X-ray images using Homomorphic Transformation and VGG inspired deep convolutional neural network. *Biocybernetics and Biomedical Engineering*, 43(1), 1–16. <https://doi.org/https://doi.org/10.1016/j.bbe.2022.11.003>
- Sun, J., Li, X., Tang, C., Wang, S.-H., & Zhang, Y.-D. (2021). MFBCNNC: Momentum factor biogeography convolutional neural network for COVID-19 detection via chest X-ray images. *Knowledge-Based Systems*, 232, 107494. <https://doi.org/https://doi.org/10.1016/j.knosys.2021.107494>
- Thakur, S., & Kumar, A. (2021). X-ray and CT-scan-based automated detection and classification of covid-19 using convolutional neural networks (CNN). *Biomedical Signal Processing and Control*, 69, 102920. <https://doi.org/https://doi.org/10.1016/j.bspc.2021.102920>
- Udayaraju, P., Narayana, T. V., Vemparala, S. H., Srinivasarao, C., & Raju, B. S. R. K. (2023). GW- CNND: Gradient weighted CNN model for diagnosing COVID-19 using radiography X-ray images. *Measurement: Sensors*, 27, 100735. <https://doi.org/https://doi.org/10.1016/j.measen.2023.100735>
- Verma, A. K., Vamsi, I., Saurabh, P., Sudha, R., G R, S., & S, R. (2021). Wavelet and deep learning-based detection of SARS-nCoV from thoracic X-ray images for rapid and efficient testing. *Expert Systems with Applications*, 185, 115650. <https://doi.org/10.1016/j.eswa.2021.115650>